Chapter 3

Steady-State Invariant Genetics: Probing the Role of Morphogen Gradient Dynamics in Developmental Patterning

Morphogen-mediated patterning is the predominant mechanism by which positional information is established during animal development. In the classical view, the interpretation of morphogen gradients is assumed to be at equilibrium and the dynamics of gradient formation are generally ignored. The problem of whether or not morphogen gradient dynamics contribute to developmental patterning has not been explored in detail, in part, because genetic experiments that selectively affect signaling dynamics while maintaining unchanged the steady-state morphogen profile are difficult to design and interpret. Here, I present a theoretical approach to identify genetic mutations in developmental patterning that may affect the transient, but leave invariant the steady-state signalling gradient. As a case study, I illustrate how these tools can be used to explore the dynamic properties of Hedgehog signaling in the developing wing of the fruit fly, *Drosophila melanogaster*. This analysis provides insights into how different properties of the Hedgehog gradient dynamics, such as the duration of exposure to the signal or the width of the gradient prior to reaching the equilibrium, can be genetically perturbed without affecting the local steady-state distribution of the gradient. I propose that this method can be generally applicable as a tool to design experiments to probe the role of transient morphogen gradients in developmental patterning and discuss potential applications of these ideas to a wide variety of problems.

3.1. Introduction

A classical paradigm in developmental biology is that cells in a developing embryo or tissue acquire information about their relative spatial location by interpreting the local concentration of chemical signals in their environment called morphogens. The key idea is that the interpretation of positional information results in the establishment of gene expression patterns whose boundaries correspond to concentration thresholds of the morphogen gradient (Wolpert, 1971; Gurdon et al., 1998; Ashe and Briscoe, 2006). A common implicit assumption of the Classical Morphogen model is that gradients are interpreted approximately at the steady state in order to produce stable patterns of gene expression (Nellen et al., 1996; Kicheva et al., 2008). However, recent quantitative imaging studies in some systems have demonstrated that morphogens are more dynamic than previously thought and have raised criticisms to the classical morphogen concept (Gregor et al., 2007; Harvey and Smith, 2009; Liberman et al., 2009). For instance, if gradient formation evolves in time, how and when are concentration thresholds interpreted? Or more generally, how do morphogen dynamics contribute to positional information? One possibility is that patterns evolve as the gradient develops, giving rise to transient patterns that converge to stable gene expression domains as the gradient approaches the equilibrium (Bourillot et al., 2002). This scenario supports a 'no-role' model for transient gradients (Fig. 3.1A), but this seems not always to be the case. For example, we recently reported that in the wing disc of the fruit fly, *Drosophila melanogaster*, the specification of different spatial domains of expression in response to Hedgehog (Hh) signalling depends on the dynamics of the Hh gradient (Nahmad and Stathopoulos, 2009). In particular, we showed that cells exposed to Hh only transiently

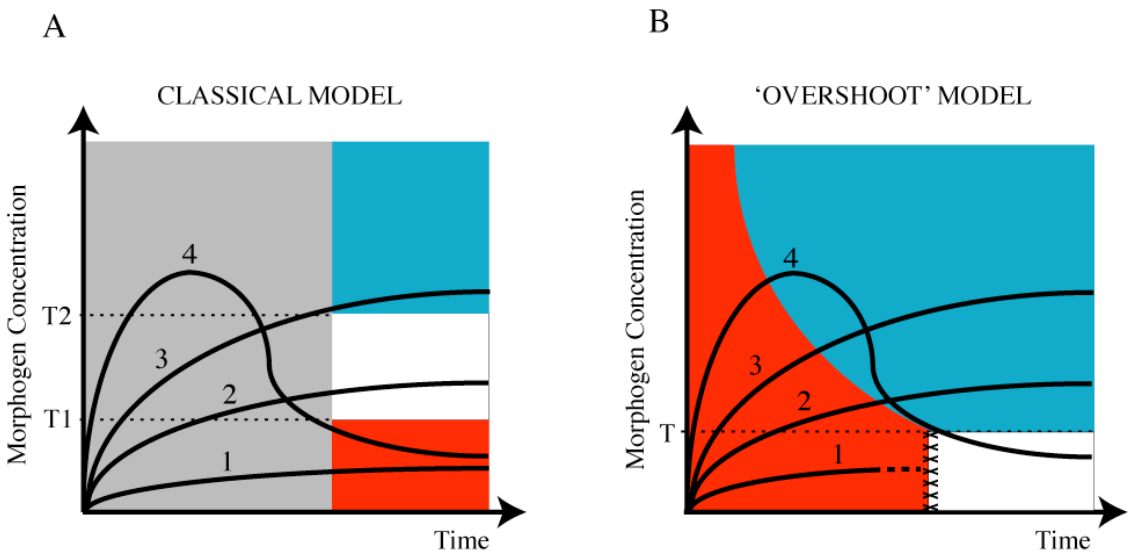

Figure 3.1 Static vs. dynamic models of morphogen-mediated patterning.

(A) In the classical view, morphogens are assumed at equilibrium and cellular states (blue, white, or red) depend on morphogen concentration thresholds (T1 and T2). In this model, the dynamics of the gradient prior to reaching the equilibrium (gray region) does not have a role in patterning. For example, cells transiently exposed to the morphogen, but that cease receiving the signal at the steady state acquire the same state (red) than cells always exposed to low signaling levels (trajectories 1 and 4). (B) In the 'Overshoot' Model (Nahmad and Stathopoulos, 2009), the dynamics of the gradient are essential for pattern formation. Cells receiving the morphogen will change from a red (OFF) to a blue (ON) state. As in (A), those cells that keep receiving the signal will maintain their blue fate (trajectories 2 and 3), but cells that lost their transient signal (trajectory 4) will adopt a different state (white) than cells that never reach the switching threshold T (trajectory 1). In (B), the red and white domains are not simple-connected, i.e. trajectories cannot cross the red-white boundary.

---

express a different combination of genes compared to cells constantly receiving the signal or cells that never receive it at all. In contrast to the Classical Morphogen Model (Fig. 3.1A), this case provides an example in which patterns are not only defined based on the steady-state readout of the morphogen concentration, but also on their history of exposure to the signal (Fig. 3.1B). In general, the problem of whether or not the dynamics of

gradient formation are required for morphogen interpretation remains largely unexplored experimentally because mutants that affect gradient dynamics are also likely to perturb the steady-state morphogen distribution. Despite the recent introduction of techniques to quantify and measure the dynamic properties of morphogen gradients in living embryos or tissues (Kicheva et al., 2007; Yu et al., 2009), the identification of mutants that selectively affect gradient dynamics with little or no effect on the equilibrium profile remains challenging.

For more than 50 years, mathematical modeling and theoretical biology have provided powerful tools to identify potential mechanisms of morphogen gradient formation and interpretation in developmental patterning (Turing, 1952; Meinhardt, 1978; von Dassow et al., 2000; Lander et al., 2002; Eldar et al., 2003; Bollenbach et al., 2008). However, much of this literature has been built on the assumption that morphogens are interpreted at the steady state and transient gradients are often completely ignored. Reducing a dynamical system to its steady state is usually mathematically convenient as the equations of the model often simplify considerably and theoretical tools are readily available to study the stability of solutions. In contrast, much less analytical tools exist to investigate the temporal evolution of a gradient and studies that have taken morphogen dynamics into consideration usually rely on exhaustive numerical explorations of high-dimensional parameter spaces (Jaeger et al., 2004; Saha and Schaffer, 2006).

In this paper, I present theoretical tools to study transients of dynamical systems in general and the role of the dynamics of morphogen gradients in particular. Given a mathematical model of a particular morphogen-based pattern formation system, we

consider parameter perturbations that may change the transient shape of a morphogen without effectively affecting its steady-state distribution. I introduce a theoretical framework to study these perturbations in a geometric way and discuss how they could be analyzed systematically. As an example, I investigate the dynamics of the Hh gradient in the *Drosophila* wing disc and show how this approach may lead to predict genetic mutants that provide insights into the role of Hh gradient dynamics during development. Other applications of these concepts and their theoretical and biological implications are also highlighted.

3.2. Methods

Wing Disc Immunostaining

In Figure 3.3A, a third instar wing disc of genotype *dpp10638/CyO* was immunostained with mouse anti-Ptc (Hybridoma Bank Developmental Studies at the University of Iowa) and rabbit anti-β-Galactosidase (Invitrogen) antisera following standard techniques. *dpp10638* is a lacZ enhancer trap reporter that expresses nuclear β-Galactosidase under the control of the *dpp* enhancer.

Analytical Solutions

The analytical solution of equation (3.1) was derived by Bergmann et al. (2007) and is given by:

$$[\mathrm{A}](x,\,t) = \mathrm{A}_0\left[\exp\left(\frac{-x}{\lambda}\right) - \frac{1}{2}\exp\left(\frac{-x}{\lambda}\right)erfc\left(\frac{\frac{2Dt}{\lambda} - x}{2\sqrt{Dt}}\right) - \frac{1}{2}\exp\left(\frac{x}{\lambda}\right)erfc\left(\frac{\frac{2Dt}{\lambda} + x}{2\sqrt{Dt}}\right)\right],$$

with *erfc*, the complementary error function, $erfc(z) = \frac{2}{\pi}\int_{z}^{\infty} \exp(-\tau^2) d\tau$. This solution was used to generate the gradient profiles in Figure 3.2C-E. An approximate analytical solution of Equation (3.6) near the AP boundary (Equation (3.8)) was obtained by linearization and the full details of this approximation are given in the Supporting Text.

Numerical Simulations

Our model of Hh-dependent patterning of the wing disc is assumed one-dimensional along the AP axis. We used a system of coordinates centered at the AP boundary (x=0) where the posterior and anterior ends of the disc were assumed at $x = -L_P$ and $x = L_A$, respectively (with L_P+L_A=200 μm, the length of the AP axis). Equations (3.5) were numerically solved with the parameters values as in Supporting Table 1 and using a Forward-in-Time-Centered-in-Space algorithm implemented in MATLAB. As in previous work (Nahmad and Stathopoulos, 2009), we use zero initial conditions, except for [*ptc*] and [Ptc] that were taken as:

$$[ptc](x, 0) = \frac{\alpha_{ptc0}}{\beta_{ptc}}, \text{ for } x > 0 \text{ and zero otherwise; } [\text{Ptc}](x, 0) = \frac{T_{\text{Ptc}}}{\beta_{\text{Ptc}}}[ptc](x, 0).$$

Furthermore, we imposed zero-flux boundary conditions at the disc extremes ($x = -L_P$; $x = L_A$), and assumed continuity of the $[\text{Hh}]_{SS}$ profile and its derivative at the AP boundary (x = 0; see Supporting Text).

3.3. Theoretical Framework: Definitions and Examples

One way to study the role of signaling dynamics is to consider perturbations that maintain certain steady-state properties of a system unchanged, but affect the history of how those

equilibrium states are reached. In this section, I introduce a general theoretical framework to define this class of perturbations, referred here as *steady-state invariant perturbations*, and use a practical example to illustrate how this approach can be used as a tool for experimental design in the context of developmental genetics.

Steady-State Invariant Perturbations: An Example

In order to introduce the concept of steady-state invariant perturbations, consider a simple example, namely, a naïve model of a one-dimensional morphogen produced at a point source (x=0) that establishes a concentration gradient by diffusion and linear degradation,

$$\frac{\partial\,[\mathrm{A}]}{\partial t} = D\frac{\partial^2[\mathrm{A}]}{\partial x^2} + \alpha\delta(x) - \beta[\mathrm{A}], \qquad (3.1)$$

where [A] denotes the concentration of morphogen A, $\delta(x)$ is the Dirac delta distribution, and α, β and D are the production, degradation, and diffusion rates of A, respectively. At the steady state, the shape of the [A] gradient is exponential* and given by

$$[\mathrm{A}]_{ss}(x) = \mathrm{A}_0 \exp\left[-\frac{x}{\lambda}\right], \qquad \text{with } \mathrm{A}_0 = \frac{\alpha}{2\sqrt{D\beta}} \text{ and } \lambda = \sqrt{\frac{D}{\beta}}. \qquad (3.2)$$

In Equation (3.2), A_0 and λ represent the amplitude and characteristic length of the steady-state gradient, and their values determine uniquely this solution. As A_0 and λ are defined in terms of the parameters of the system, a perturbation on the wild-type parameter values will maintain the steady-state solution invariant if and only if the values of A_0 and λ remain unchanged. To formalize, let $(\tilde{\alpha}, \tilde{\beta}, \tilde{D})$ be the wild-type parameter values and consider a mutant that perturbs the system such that the effective parameter

* In this example, we ignore boundary conditions by assuming that the system is infinitely long and diffusion occurs in both directions from the source. These assumptions allow us to solve the full time-dependent problem (3.1) exactly using the method of Fourier transforms (Bergmann et al., 2007; see Methods section) and solution (3.2) arises as a limit of the time-dependent solution when $t \to \infty$.

values of the system change to (α', β', D'). We say that the mutant preserves the steady-state gradient or is *steady-state invariant* if the following equations hold:

$$\frac{\alpha'}{\sqrt{D'\beta'}} = \frac{\tilde{\alpha}}{\sqrt{\tilde{D}\tilde{\beta}}} \equiv \text{constant1}$$
$$\sqrt{\frac{D'}{\beta'}} = \sqrt{\frac{\tilde{D}}{\tilde{\beta}}} \equiv \text{constant2}. \qquad (3.3)$$

The set of all steady-state invariant perturbations can be represented geometrically in parameter space and will be referred to as the *steady-state invariant set* of the system. In general, a steady-state invariant perturbation Δ can be denoted as a vector in parameter space that is based on the point of wild-type parameter values and ends on the steady-state invariant set (Fig. 3.2A). In this example, it follows that any perturbed parameter vector (α', β', D') satisfying Equation (2.3) must be of the form,

$$(\alpha', \beta', D') = (\delta\tilde{\alpha}, \delta\tilde{\beta}, \delta\tilde{D}) \quad \text{for some } \delta > 0. \qquad (3.4)$$

Equation (3.4) represents a straight line in parameter space that crosses through the origin and contains the wild-type parameter vector ($\tilde{\alpha}$, $\tilde{\beta}$, $\tilde{D}$) (Fig. 3.2B). Thus, the line defined by Equation (3.4) is the steady-state invariant set of this system. Importantly, a perturbation that keeps the parameter values within the steady-state invariant set may affect the transient evolution of the gradient but maintains the steady-state morphogen gradient unchanged. In this simple example, the effects on morphogen dynamics along the steady-state invariant set are simple to interpret; for $\delta < 1$, gradient formation is slower compared to the wild-type case, while for $\delta > 1$ the steady-state gradient is approached faster than in the wild type (Fig. 3.2C-E). In addition, the rates in which the steady state is approached are space-dependent; cells adjacent to the source approach equilibrium faster than cells away from it and this property also holds after steady-state

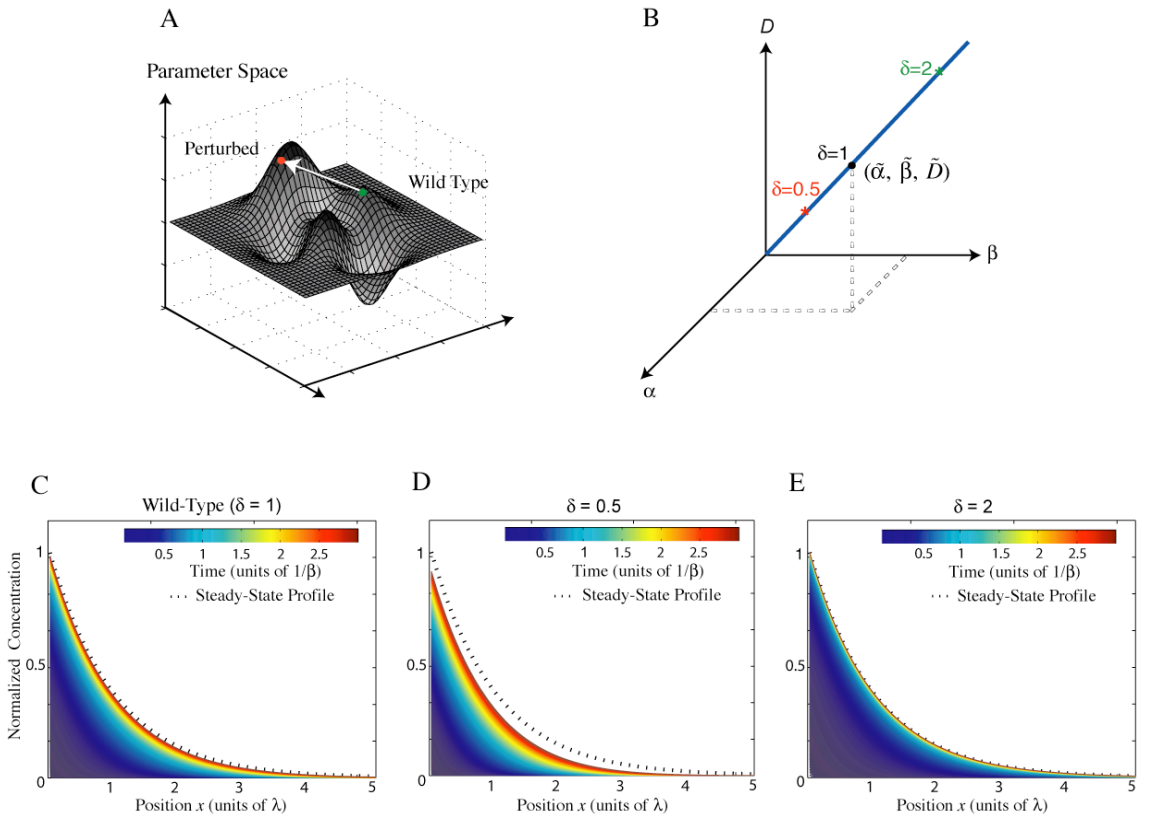

Figure 3.2 Analysis of steady-state invariant perturbations in the case of a morphogen established by diffusion and uniform linear degradation.

(A) Steady-state invariant sets can be generally described as subsets of parameter space. A steady-state invariant perturbation is represented by a vector in parameter set based on the point of wild-type parameter values (green) and ending on another point of the steady-state invariant set (red). (B) The steady-state invariant set of the morphogen modelled by Equation (1) is the straight line defined by Equation (3.4) with δ>0. (C-E) Temporal dynamics of the morphogen concentration [from Equation (3.1)] when parameter values α, β, and D are perturbed along the steady-state invariant set by varying the value of δ. (C) δ=1 (unperturbed case); (D) δ=0.5; (E) δ=2. For comparison purposes, gradients in (C-E) are plotted using the same colour-coded timescale and the (invariant) steady-state profile is displayed in all three panels.

---

invariant perturbations (see Supporting Fig. 3.1). Despite the simplicity of this example, the definition of steady-state invariant sets and the method to compute them can be generalized (see Box 3.1).

BOX 3.1

Consider the following general model of developmental patterning. Let $\mathbf{G}=([g_1], [g_2], \ldots, [g_k])$ a vector denoting concentrations of gene products $g_1, \ldots, g_k$ and assume that the dynamics of gene concentrations is described by a reaction-diffusion equation of the form

$$\frac{\partial \mathbf{G}}{\partial t} = \mathbf{D}\nabla^2\mathbf{G} + \boldsymbol{f}(\mathbf{G}, \boldsymbol{\mu}). \qquad \text{(B1)}$$

In this equation, ∇^2 denotes the Laplacian operator ($\nabla^2 \equiv \frac{\partial^2}{\partial x^2} + \frac{\partial^2}{\partial y^2} + \frac{\partial^2}{\partial z^2}$), $\mathbf{D}$ is a vector of diffusion coefficients, $\boldsymbol{f}$ is the reaction function that describes the interactions of gene products, and $\mathbf{m}$ is a vector of kinetic rates or parameters of the system. Note that the systems considered in the text (Equations (3.1) and (3.5)) are particular cases of Equation (B1). At the steady state, we set the time derivatives to zero so that the steady-state concentrations, $\mathbf{G}^{ss}$, obey the following equation,

$$0 = \mathbf{D}\nabla^2\mathbf{G}^{SS} + \boldsymbol{f}(\mathbf{G}^{SS}, \boldsymbol{\mu}). \qquad \text{(B2)}$$

Assume that the solution of (B2) exists and let us denote it as $\mathbf{G}_{\mathbf{x}}^{SS}(\boldsymbol{\mu})$.

A parameter perturbation (e.g., a genetic perturbation) of the system is a function D of the form $D(\mathbf{m})=(d_1m_1, d_1m_2, \ldots, d_rm_r) \equiv (\mu'_1, \mu'_2, \ldots, \mu'_r)$ for some positive constants $d_1, \ldots, d_r$. We are interested in the study of perturbations that leave the steady-state solution $\mathbf{G}_{\mathbf{x}}^{SS}(\boldsymbol{\mu})$ unchanged at least in a region of space **S**. A *steady-state invariant perturbation* is a parameter perturbation D that satisfies the following property:

$$\mathbf{G}_{\mathbf{x}}^{SS}(\boldsymbol{\mu}) = \mathbf{G}_{\mathbf{x}}^{SS}(\Delta(\boldsymbol{\mu})) \qquad \text{for all } \mathbf{x} \in \mathbf{S}. \qquad \text{(B3)}$$

Our goal is to find the set of steady-state invariant perturbations satisfying Equation (B3). For this purpose, it is useful to consider the following geometric representation. Note that there is a one-to-one correspondence between parameter perturbations and points in parameter space (i.e points of the form $(\mu'_1, \mu'_2, \ldots, \mu'_r)$ with $m'_i \geq 0$, i=1,…, r). For each **x** (fixed), $\mathbf{G}_{\mathbf{x}}^{SS}(\boldsymbol{\mu}) = \text{constant}$ and therefore, we can consider the points $(\mu'_1, \mu'_2, \ldots, \mu'_r)$ in parameter space that satisfy

$$\mathbf{G}_{\mathbf{x}}^{SS}(\mu'_1, \mu'_2, \ldots, \mu'_r) = \mathbf{G}_{\mathbf{x}}^{SS}(\boldsymbol{\mu}) = \text{constant}, \qquad \text{for } \mathbf{x} \text{ fixed}. \qquad \text{(B4)}$$

Denote by $W_{\mathbf{x}}$ the set of points in parameter space satisfying (B4) for a given **x**, and define the *steady-state invariant set,* **W**, of the system (in **S**) as the set that results from the intersection of $W_{\mathbf{x}}$ for all $\mathbf{x} \in \mathbf{S}$, i.e.

$$\Omega = \bigcap_{\mathbf{x} \in \mathbf{S}} \Omega_{\mathbf{x}}, \qquad \text{(B5)}$$

(see Supporting Figure 3.2). Hence, the steady-state invariant set is a geometric representation of the set of mutants that leave invariant the equilibrium gene concentrations in cells located within the region **S**.

Hh Signaling in the *Drosophila* Wing Disc: A Case Study

In order to motivate the applications of the concept of steady-state invariant sets to practical cases, the dynamic properties of Hh signaling in the *Drosophila* wing imaginal disc were investigated. In a recent study, we provided experimental evidence for the existence of a transient expansion (or 'overshoot') of the Hh gradient in the *Drosophila* wing disc which is required to define three different regions of signal exposure (Fig. 3.3A; Nahmad and Stathopoulos, 2009). However, how specific properties of this transient overshoot (e.g., its duration) contribute to patterning has not been established. Here, I use the concept of steady-state invariant perturbations to make predictions about which genetic perturbations of the system may affect the dynamic properties of this overshoot without affecting the equilibrium profile of the gradient.

Consider the mathematical model of the Hh signaling pathway originally presented in Nahmad and Stathopoulos (2009):

$$
\begin{aligned}
\frac{\partial[\mathrm{Hh}]}{\partial t} &= D\frac{\partial^2[\mathrm{Hh}]}{\partial x^2} + S^{-}(x)\alpha_{\mathrm{Hh}} - \gamma_{\mathrm{Hh\_Ptc}}[\mathrm{Hh}][\mathrm{Ptc}] - \beta_{\mathrm{Hh}}[\mathrm{Hh}] \\
\frac{\partial[ptc]}{\partial t} &= S^{+}(x)\alpha_{ptc0} + \frac{\alpha_{ptc}[\mathrm{Signal}]^{\mathrm{m}}}{k_{ptc}^{\mathrm{m}} + [\mathrm{Signal}]^{\mathrm{m}}} - \beta_{ptc}[ptc] \\
\frac{\partial[\mathrm{Ptc}]}{\partial t} &= T_{\mathrm{Ptc}}[ptc] - \gamma_{\mathrm{Hh\_Ptc}}[\mathrm{Hh}][\mathrm{Ptc}] - \beta_{\mathrm{Ptc}}[\mathrm{Ptc}] \\
\frac{\partial[\mathrm{Hh\_Ptc}]}{\partial t} &= \gamma_{\mathrm{Hh\_Ptc}}[\mathrm{Hh}][\mathrm{Ptc}] - \beta_{\mathrm{Hh\_Ptc}}[\mathrm{Hh\_Ptc}] \\
\frac{\partial[\mathrm{Signal}]}{\partial t} &= \frac{S^{+}(x)\alpha_{\mathrm{Signal}}\left(\frac{[\mathrm{Hh\_Ptc}]}{[\mathrm{Ptc}]}\right)^{\mathrm{n}}}{k_{\mathrm{Signal}}^{\mathrm{n}} + \left(\frac{[\mathrm{Hh\_Ptc}]}{[\mathrm{Ptc}]}\right)^{\mathrm{n}}} - \beta_{\mathrm{Signal}}[\mathrm{Signal}],
\end{aligned}
\tag{3.5}
$$

where [Hh], [*ptc*], [Ptc], [Hh_Ptc] are the concentrations of Hh, *ptc* (mRNA), Ptc (protein), and the Hh-Ptc complex, respectively. The coefficients α, β, γ, and T,

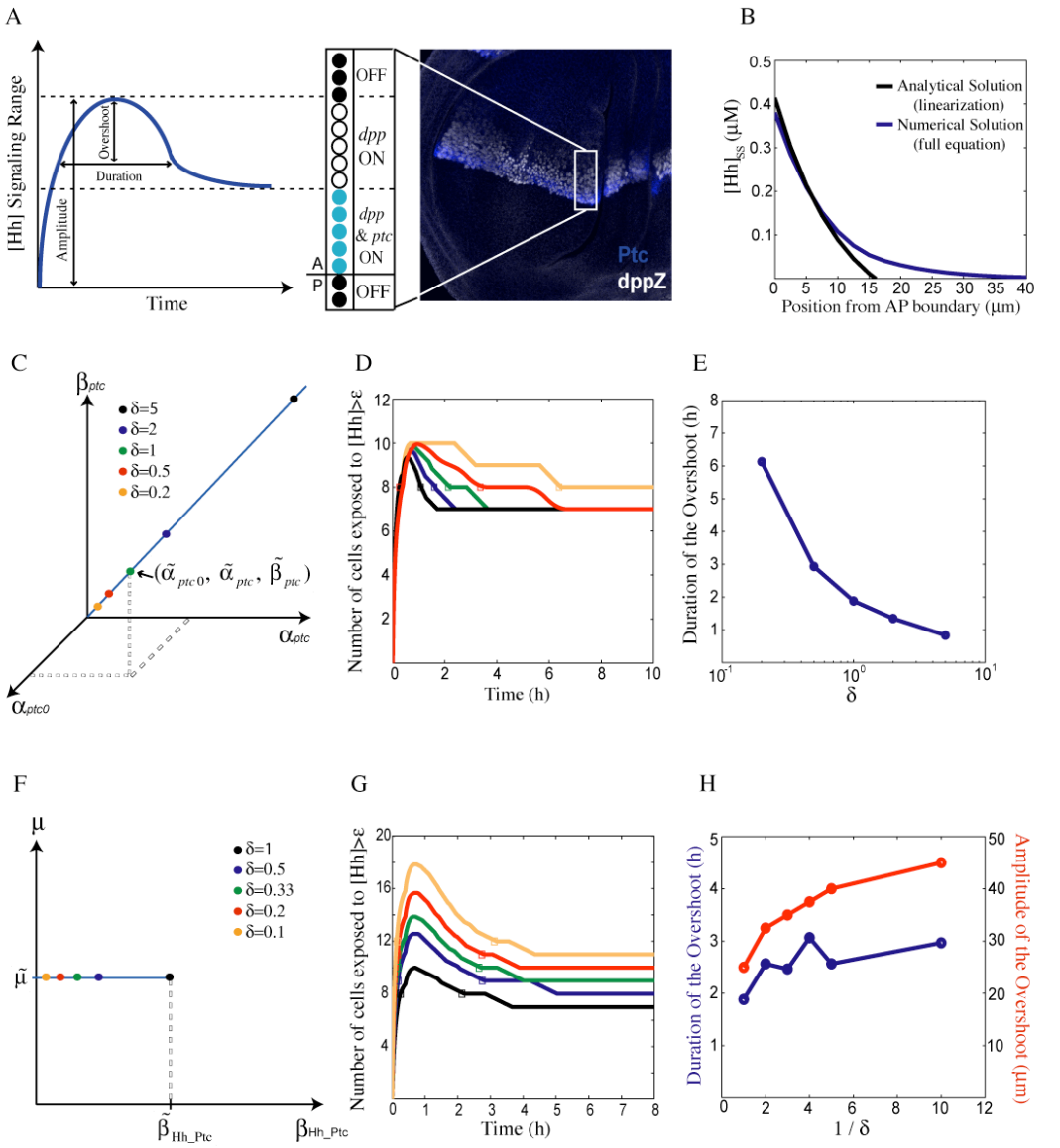

Figure 3.3 Analysis of steady-state invariant perturbations of the Hh morphogen in the *Drosophila* wing disc.

(A) Summary of the 'Overshoot' Model (Nahmad and Stathopoulos, 2009). An overshoot of the Hh gradient determines patterning of the *Drosophila* wing disc. Three gene expression domains are established by this overshoot. Cells that do not receive the signal or that receive sustained signalling levels are denoted by red and blue, respectively. Certain cells that are only transiently exposed to the signal are denoted by the white state and characterized by *dpp* (but not *ptc*) expression. The photo displays wild-type expression patterns of *ptc* and *dpp* in a third-instar wing disc (with the anterior compartment oriented upwards) carrying a *dpp*-lacZ reporter immunostained using Ptc (blue) and β-Galactosidase (white) antibodies. (B)

Comparison of the Hh steady-state profiles as obtained from the numerical solution of equation (6) or the exact solution of the linearization [Equation (3.8)]. Note that the approximation is good only near the AP boundary. (C) The steady-state invariant subset described by equation (3.10) represents a line parameterised by the variable δ. (*d*) Analysis of the overshoot in selected steady-state invariant mutants. Colour coding of the curves correspond to different values of δ as shown in (C). Note that the amplitude of the overshoot is unaffected by these steady-state invariant perturbations. (E) The duration of the overshoot (in hours) as extracted from (D) (squares) as a function of δ. (F) Representation of the steady-state invariant subset from equation (11) in two dimensions. The vertical axis denoted by μ, represents any other dimensions of parameter space. (G) Similar analysis as in (D), but corresponding to the approximate steady-state invariant subset in (F). (H) Steady-state invariant perturbations in (F) considerably affect the amplitude (red), but not the duration of the overshoot (blue).

---

represent the rates of synthesis, degradation, complex formation, and translation, respectively. $S^+(x)$ (or $S^-(x)$) is a step function of the form $S^+(x) = 1$ if $x > 0$ (or $S^-(x) = 1$ if $x < 0$), and zero otherwise that is used to represent compartment-specific reactions. For example, in this model, extracellular Hh is produced in the posterior compartment ($x<0$) and diffuses across the anterior-posterior (AP) boundary ($x=0$). In the anterior compartment ($x>0$), Hh binds its receptor, Patched (Ptc), and Hh signaling is activated as a function of the ratio of bound to unbound receptor concentrations (Casali and Struhl, 2004). As in our previous study, the variable [Signal] denotes the concentration of a factor that models pathway activity at the intracellular level (see Nahmad and Stathopoulos (2009) for further details). At the steady state, the set of Equations (3.5) reduce to the following second-order equation, only valid within the anterior compartment ($x>0$),

$$D\frac{d^2[\mathrm{Hh}]_{\mathrm{ss}}}{dx^2}-\frac{\chi\,[\mathrm{Hh}]_{\mathrm{ss}}}{\beta_{\mathrm{Ptc}}+\gamma_{\mathrm{Hh\_Ptc}}[\mathrm{Hh}]_{\mathrm{ss}}}\left[\alpha_{ptc0}+\frac{\alpha_{ptc}[\mathrm{Hh}]_{\mathrm{ss}}^{nm}}{\eta\left[\kappa^n+[\mathrm{Hh}]_{\mathrm{ss}}^n\right]^m+[\mathrm{Hh}]_{\mathrm{ss}}^{nm}}\right]-\beta_{\mathrm{Hh}}[\mathrm{Hh}]_{\mathrm{ss}}=0, \qquad (3.6)$$

with $\chi=\frac{T_{\mathrm{Ptc}}\gamma_{\mathrm{Hh\_Ptc}}}{\beta_{ptc}}$, $\kappa=\frac{k_{\mathrm{Signal}}\beta_{\mathrm{Hh\_Ptc}}}{\gamma_{\mathrm{Hh\_Ptc}}}$, and $\eta=\frac{k_{ptc}\beta_{\mathrm{Signal}}}{\alpha_{\mathrm{Signal}}}$. This equation is nonlinear and an analytical solution may be difficult (or impossible) to obtain. However, near the anterior-posterior boundary ($0< x <<1$), we can assume that Hh exists at sufficiently high levels so that $[\mathrm{Hh}]_{\mathrm{SS}}^{\mathrm{n}} >> \kappa^{\mathrm{n}}$ holds in this region (see parameter values in Supporting Table 1). Under this assumption, one of the nonlinear terms in Equation (3.6) can be approximated by a constant,

$$\frac{\alpha_{ptc}[\mathrm{Hh}]_{\mathrm{ss}}^{nm}}{\eta\left[\kappa^n+[\mathrm{Hh}]_{\mathrm{ss}}^n\right]^m+[\mathrm{Hh}]_{\mathrm{ss}}^{nm}}\approx\frac{\alpha_{ptc}}{\eta+1}.$$

The other nonlinear term in Equation (2.6) can be linearized (via a Taylor expansion) around a point where the condition $[\mathrm{Hh}]_{\mathrm{SS}}^{\mathrm{n}} >> \kappa^{\mathrm{n}}$ is satisfied (see details in the Supporting Text). Under these approximations, it can be shown that near to the AP boundary the steady-state gradient can be approximately modeled by the following linear equation:

$$\frac{d^2[\mathrm{Hh}]_{\mathrm{SS}}}{dx^2}-\mathrm{B}[\mathrm{Hh}]_{\mathrm{SS}}-\mathrm{C}=0, \qquad (3.7)$$

with

$$\mathrm{B}=\frac{\beta_{\mathrm{Hh}}}{D}\left[1+\frac{T_{\mathrm{Ptc}}\gamma_{\mathrm{Hh\_Ptc}}}{\beta_{ptc}\left(3\beta_{\mathrm{Hh}}\beta_{\mathrm{Ptc}}+\gamma_{\mathrm{Hh\_Ptc}}\alpha_{\mathrm{Hh}}\right)}\left(\alpha_{ptc0}+\frac{\alpha_{ptc}\alpha_{\mathrm{Signal}}}{\alpha_{\mathrm{Signal}}+k_{ptc}\beta_{\mathrm{Signal}}}\right)\left(3-\frac{\gamma_{\mathrm{Hh\_Ptc}}\alpha_{\mathrm{Hh}}}{3\beta_{\mathrm{Hh}}\beta_{\mathrm{Ptc}}+\gamma_{\mathrm{Hh\_Ptc}}\alpha_{\mathrm{Hh}}}\right)\right]$$

and $\mathrm{C}=\frac{3\beta_{\mathrm{Hh}}T_{\mathrm{Ptc}}\gamma_{\mathrm{Hh\_Ptc}}^2\alpha_{\mathrm{Hh}}^2}{\beta_{ptc}D\left(3\beta_{\mathrm{Hh}}\beta_{\mathrm{Ptc}}+\gamma_{\mathrm{Hh\_Ptc}}\alpha_{\mathrm{Hh}}\right)^2}\left(\alpha_{ptc0}+\frac{\alpha_{ptc}\alpha_{\mathrm{Signal}}}{\alpha_{\mathrm{Signal}}+k_{ptc}\beta_{\mathrm{Signal}}}\right)$ (see Supporting Text for

details). Using appropriate boundary conditions (see Methods section), the solution of Equation (3.7) is given by:

$$[\mathrm{Hh}]_{\mathrm{SS}}(x) = \mathrm{A}\exp\left[-\sqrt{\mathrm{B}}x\right] - \frac{\mathrm{C}}{\mathrm{B}}, \qquad (3.8)$$

with $\mathrm{A} = \dfrac{\dfrac{\alpha_{\mathrm{Hh}}}{\beta_{\mathrm{Hh}}} + \dfrac{\mathrm{C}}{\mathrm{B}}}{1 + \sqrt{\dfrac{\mathrm{B}D}{\beta_{\mathrm{Hh}}}}\coth\left(\sqrt{\dfrac{\beta_{\mathrm{Hh}}}{D}}L_{\mathrm{P}}\right)}$ and L_{P} is the width of the posterior compartment (see Supporting Text). In fact, the numerical solution of Equation (3.6) (using the parameters values in Supporting Table 2.1) is well approximated by the exact solution of the linearization [Equation (3.8)] close to the anterior-posterior boundary (Fig. 3.3B). A steady-state perturbation will maintain the Hh gradient approximately invariant near the anterior-posterior boundary if Equation (3.8) is unaffected by the perturbation, this is, if A, $\sqrt{\mathrm{B}}$, and $\dfrac{\mathrm{C}}{\mathrm{B}}$ remain constant. Thus, under these approximations, the steady-state invariant set of the linearized system is given by:

$$\mathrm{B}' = \frac{\beta'_{\mathrm{Hh}}}{D'}\left[1 + \frac{T'_{\mathrm{Ptc}}\gamma'_{\mathrm{Hh\_Ptc}}\zeta'}{\beta'_{ptc}\left(3\beta'_{\mathrm{Hh}}\beta'_{\mathrm{Ptc}} + \gamma'_{\mathrm{Hh\_Ptc}}\alpha'_{\mathrm{Hh}}\right)}\left(3 - \frac{\gamma'_{\mathrm{Hh\_Ptc}}\alpha'_{\mathrm{Hh}}}{3\beta'_{\mathrm{Hh}}\beta'_{\mathrm{Ptc}} + \gamma'_{\mathrm{Hh\_Ptc}}\alpha'_{\mathrm{Hh}}}\right)\right] = \text{constant1}$$

$$\mathrm{C}' = \frac{3\beta'_{\mathrm{Hh}}T'_{\mathrm{Ptc}}\gamma'^{2}_{\mathrm{Hh\_Ptc}}\alpha'^{2}_{\mathrm{Hh}}\zeta'}{\beta'_{ptc}D'\left(3\beta'_{\mathrm{Hh}}\beta'_{\mathrm{Ptc}} + \gamma'_{\mathrm{Hh\_Ptc}}\alpha'_{\mathrm{Hh}}\right)^{2}} = \text{constant2} \qquad (3.9)$$

$$\mathrm{A}' = \frac{\dfrac{\alpha'_{\mathrm{Hh}}}{\beta'_{\mathrm{Hh}}} + \dfrac{\mathrm{C}'}{\mathrm{B}'}}{1 + \sqrt{\dfrac{D'\,\mathrm{B}'}{\beta'_{\mathrm{Hh}}}}\coth\left(\sqrt{\dfrac{\beta'_{\mathrm{Hh}}}{D'}}L_{\mathrm{P}}\right)} = \text{constant3},$$

where constant1, constant2, and constant3 are given by the wild-type parameter values and $\zeta' = \alpha'_{ptc0} + \dfrac{\alpha'_{ptc}\alpha'_{\mathrm{Signal}}}{\alpha'_{\mathrm{Signal}} + k'_{ptc}\beta'_{\mathrm{Signal}}}$. Although any set of perturbed parameter values that satisfy these equations will maintain the approximated steady-state gradient unchanged,

the steady-state invariant set defined by Equations (3.9) is not very useful in practice because it involves more than fifteen parameters. Therefore, it is convenient to study particular subsets of the set defined by Equations (3.9). As a first case, consider,

$$(\alpha'_{ptc},\alpha'_{ptc},\beta'_{ptc}) = (\delta\tilde{\alpha}_{ptc0},\delta\tilde{\alpha}_{ptc},\delta\tilde{\beta}_{ptc}), \quad \text{for any } \delta > 0 \qquad (3.10)$$

with $\tilde{\alpha}_{ptc0}$, $\tilde{\alpha}_{ptc}$, and $\tilde{\beta}_{ptc}$ denoting the wild-type parameter values and all other parameters kept unperturbed (i.e. at their wild-type values). By substitution into Equations (3.9), it is clear that Equation (3.10) represents a steady-state invariant subset of the linearized system. In fact, Equation (3.10) also leaves invariant the original steady-state equation of the system [Equation (3.6)] and therefore, it is an exact steady-state invariant subset of the system. Geometrically, Equation (3.10) represents a line in the α_{ptc0}–α_{ptc}–β_{ptc} parameter subspace (Fig. 3.3C). Numerical simulations suggest that a few-fold changes in δ affect the duration but have little effect in the amplitude of the overshoot (Fig. 3.3D,E). In particular, we noted that the duration of the overshoot increases rapidly as δ decreases (δ<1), but decreases slowly as δ increases (δ >1). Therefore, perturbations along this steady-state invariant subset provide the opportunity to study the role of signal duration in more detail.

An even simpler case of a steady-state invariant subset of the linearized system can be obtained by noticing that the system of Equations (3.9) does not involve the degradation rate of the Hh-Ptc complex, $\beta_{\text{Hh\_Ptc}}$. Therefore, under these approximations, the steady-state solution does not depend on the value of $\beta_{\text{Hh\_Ptc}}$. For simplicity, consider the approximate steady-state invariant subset given by:

$$\beta'_{\text{Hh\_Ptc}} = \delta\tilde{\beta}_{\text{Hh\_Ptc}}, \qquad \text{for } 0<\delta<1 \qquad (3.11)$$

with all other parameters held constant at their wild-type values (Fig. 3.3F). The constraint $0< \delta <1$ was enforced so that the assumption $[Hh]^n_{SS} >> \kappa^n$ remains valid. In contrast to the subset defined by Equation (3.10), perturbations along the subset described by Equation (3.11) will affect the amplitude of the overshoot, but its duration will be maintained relatively constant (Fig. 3.3G,H). The simplicity of this subset permits the design of a genetic steady-state invariant perturbation. The *ptc*^{14} allele has been characterized as a mutant that is defective in endocytosis-dependent internalization and degradation of the Hh-Ptc complex, suggesting that the stability of the Hh-Ptc complex is increased in Ptc^{14} mutants (Torroja et al., 2004). Importantly, other properties of the Ptc protein appear unaffected in *ptc*^{14} mutant clones. For example, Ptc^{14} proteins bind Hh and repress Hh signal transduction in a similar manner than wild-type Ptc (Torroja et al., 2004). Furthermore, Ptc^{14} is not over expressed in anterior clones away from the AP boundary, suggesting that unbound Ptc^{14} degradation is normal. This genetic evidence suggests that β_{Hh_Ptc} decreases in *ptc*^{14} mutants, while other parameters approximately maintain their wild-type values. Therefore, we predict that *ptc*^{14} mutants satisfy Equation (3.11) and can be considered as a steady-state invariant perturbation of the system near the AP boundary. Based on our modeling results, perturbations along this steady-state invariant subset affect the amplitude of the overshoot, but not the overall shape and duration of the transient response suggesting that more anterior cells would be transiently exposed to the signal (Fig. 3.3G,H). Experiments using *ptc*^{14} mutant clones abutting the anterior-posterior show that the expression domains of Hh target genes expand in the region of these clones (Torroja et al., 2004), consistent with the predictions of our model and our simulations (Nahmad and Stathopoulos, 2009; Fig. 3.3G).

Other subsets can be similarly obtained from Equations (3.9) and their effects on transient dynamics can be systematically analyzed. However, sets involving more parameters are difficult to visualize and perturbations along these subsets may not be easily achieved by experimental manipulations (see below).

3.4 Analysis of Steady-State Invariant Sets

The problem of computing the steady-state invariant set from a given model is in general non-trivial. Although the example of the single morphogen gradient established by diffusion and degradation [Equation (3.1)] is not intended to represent any biological morphogen of interest, it was chosen because the steady-state invariant set can be computed exactly. However, in most cases a solution to the steady-state problem (equation (B2) in Box 3.1) cannot be obtained analytically. Nonetheless, there are different manners to overcome this problem and get a partial or approximate set of steady-state invariant perturbations. One easy way to obtain at least a steady-state invariant subset of a system is to simply inspect the steady-state equation and ask which parameter perturbations leave the equation invariant. For example, perturbations that satisfy Equation (3.10) leave the steady-state problem [Equation (3.6)] unchanged. In this case, there is no need to know the solution of the steady-state equation, but in general, this approach will only provide a subset of steady-state invariant perturbations. We will say that a steady-state invariant set is *direct* if it can be deduced from the steady-state equation. Note that Equation (3.4) is a direct subset of Equation (3.1), and from the steady-state solution (3.2), we verified that it contains all the steady-state invariant perturbations of the system. But this is not true in general. An interesting theoretical

challenge for the future will be to find conditions to determine in which cases the full steady-state invariant set is direct, i.e., when we can obtain all steady-state invariant perturbations of the system without the need of solving the equations.

Alternatively, as we did for Equation (3.6), an approximate steady-state invariant set can be obtained by linearization. One advantage of this approach is that subsets may be more simple and useful for experiment design (e.g., Equation (3.11)). However, unlike exact steady-state invariant sets that are valid throughout the developing field, these approximations are rather local (Fig. 3.3B).

Finally, another approach is to compute the exact steady-state invariant set by spatially discretizing the system, i.e., turning the problem (Equation (B1) in Box 3.1) into a system of ordinary differential equations. In fact, this is the way in which we defined steady-state invariant sets in general in Box 3.1. Using this approach, the property of steady-state invariance needs not to be global, i.e., it can be considered in a desired subset of the whole developmental field and this might often be convenient in practice. For example, some genetic perturbations are lethal to the organism, but can be studied in a specific developmental context (e.g., using mosaic genetic analysis). Another advantage is that embryos and tissues are composed by discrete entities (cells), so that modelling the system in this way might be well justified in this kind of problem.

In practice, it would be convenient to know, based on the geometry of the steady-state invariant set, how difficult is to design a genetic experiment that causes a steady-state invariant perturbation in the system. In other words, how likely is it for a random parameter perturbation to be steady-state invariant? A geometric notion that provides

insight into this question is the concept of codimension*. Intuitively, the codimension of a geometric set tells us how large the dimension of space where the set is embedded is compared to the dimension of the set. For example, the codimension of a sphere is one in a three-dimensional space, but n-2 if considered in a space of dimension n. For the practical purposes of this study, we define the codimension of a set as follows. Let M be a steady-state invariant set that affects *s* parameters and can be parameterized by *r* variables, then the codimension of M is defined as *codim*(M)=*s*-*r*. For instance, the steady-state invariant subsets defined by Equations (3.10) and (3.11) depend on three (α_{ptc0}, α_{ptc}, and β_{ptc}) and one ($\beta_{\mathrm{Hh\_Ptc}}$) parameters, respectively, and both are parameterized by the single variable δ. Therefore, their codimensions are two and zero, respectively. Intuitively, the codimension of a set is inversely related to the concept of *degrees of freedom*, i.e., the number of parameters that can be arbitrarily varied without abandoning the set. In general, steady-state invariant sets of small codimensions (or large degrees of freedom) would be expected to be more suitable in practice because they provide further flexibility in generating steady-state invariant perturbations. The extreme scenario is when the codimension is zero and any perturbation of the parameters involved is in fact steady-state invariant. This scenario is potentially very useful for experimental design because such perturbations do not require precise tuning of parameter values. For example, the fact that the codimension of the subset defined by Equation (3.11) is zero allowed us to propose a concrete experiment (using the ptc^{14} allele) to locally introduce steady-state invariant perturbations in this system.

* Steady-state invariant sets are defined by algebraic equations and therefore the concepts of dimension and codimension can be rigorously defined (see Supporting Text).

3.5 Concluding Remarks

There is recently much interest in the problem of how the dynamics of morphogen gradients contribute to developmental patterning (reviewed by Kutejova et al., 2009). In this paper, I presented a general theoretical approach that may help to identify mutations that affect the transient establishment of morphogen gradients without changing their equilibrium distribution. Although the experimental implementation of these tools to study the role of morphogen gradient dynamics in developmental pattern formation is left to future studies, I provided details of how they can be implemented in practical systems. In particular, the analysis of steady-state invariant subsets in a model of Hh signalling in the *Drosophila* wing provides the opportunity to decouple two properties of the Hh gradient overshoot, namely, duration and amplitude. The duration of the overshoot can be modulated in a steady-state invariant manner by varying the rates of *ptc* production and degradation (Fig. 3.3C-E). Furthermore, the amplitude of the overshoot can be affected by reducing the rate of Ptc-dependent Hh internalization and degradation. In fact, previous experiments in which a mutant form of Ptc (Ptc^{14}), that is defective in Ptc-mediated Hh endocytosis, but otherwise appears to function normally, provides an example of an experimental steady-state invariant perturbation in this system.

Another interesting application of these tools is to consider steady-state invariant sets as parameter perturbations to which the system exhibits robustness. For instance, in engineering it is often desirable to design systems in which the steady state is robust to a certain class of perturbations. Therefore, the converse problem, namely, to construct a dynamical system that will maintain a desired set of perturbations invariant poses an interesting challenge for the future. The context in which the converse problem has been

studied in some detail is robust control theory and there are several examples in which imposing invariance into the steady-state values of some variables constrains the dynamic properties of the system. One of the most studied examples is 'perfect adaptation' in bacterial chemotaxis (Barkai and Leibler, 1997; Alon et al., 1999). For instance, a well-known result in control theory is that the steady-state error in some desired signal remains negligible despite external perturbations or variations in internal components if and only if the error dynamics are governed by integral feedback and this has been shown to apply to perfect adaptation in chemotaxis (Yi et al., 2000). Furthermore, a recent report provides structural conditions on biochemical reaction network dynamics to guarantee invariance of particular steady-state concentrations (Shinar and Feinberg, 2010). Finally, it is likely that evolution has faced and solved this converse problem in selecting for optimal mechanisms for developmental patterning; in some systems, it is possible that natural selection has minimized the effects of certain classes of genetic perturbations to maintain invariant some essential gene expression patterns. Alternatively, natural selection may have taken advantage of the diversity of morphogen dynamics to evolve the mechanisms of developmental pattern formation.

3.6 Outlook

It is broadly recognized that physics and engineering have not only clearly benefited from mathematics, but also have substantially motivated the development of new mathematical theories and concepts. Although the use of mathematical modelling has become a common practice in biological research in general, and in developmental biology in particular (Tomlin and Axelrod, 2007; Ibañes and Izpisúa-Belmonte, 2008; Oates et al.,

2009), some theoreticians hope that problems in biology will contribute to the development of new mathematics in the 21st century (Cohen, 2004; Sturmfels, 2005). The theory of steady-state invariant sets introduced here was motivated by the problem of whether or not morphogen dynamics contribute to developmental patterning. Nonetheless, the applications of the tools presented here are not limited to the design of experimental perturbations and/or to test the role of transient signals in developmental patterning, but may be broadly applicable to a large class of problems and will hopefully depict interesting research avenues in dynamical systems theory.